Available online at www.sciencedirect.com
ScienceDirect
Remote Sensing of Environment 105 (2006) 129–141
Remote Sensing of Environment
www.elsevier.com/locate/rse

Intra- and inter-class spectral variability of tropical tree species at La Selva, Costa Rica: Implications for species identification using HYDICE imagery

Jinkai Zhang, Benoit Rivard *, Arturo Sánchez-Azofeifa, Karen Castro-Esau

Earth Observation Systems Laboratory (EOSL), Department of Earth and Atmospheric Sciences, University of Alberta, Edmonton, Alberta, Canada T6G 2E3

Received 16 June 2005; received in revised form 19 June 2006; accepted 19 June 2006

Abstract

Hyperspectral remote sensing provides great potential to monitor and study biodiversity of tropical forests through species identification and mapping. In this study, five species were selected to examine crown-level spectral variation within and between species using HYperspectral Digital Collection Experiment (HYDICE) data collected over La Selva, Costa Rica. Spectral angle was used to evaluate the spectral variation in reflectance, first derivative and wavelet-transformed spectral domains. Results indicated that intra-crown spectral variation does not always follow a normal distribution and can vary from crown to crown, therefore presenting challenges to statistically define the spectral variation within species using conventional classification approaches that assume normal distributions. Although derivative analysis has been used extensively in hyperspectral remote sensing of vegetation, our results suggest that it might not be optimal for species identification in tropical forestry using airborne hyperspectral data. The wavelet-transformed spectra, however, were useful for the identification of tree species. The wavelet coefficients at coarse spectral scales and the wavelet energy feature are more capable of reducing variation within crowns/species and capturing spectral differences between species. The implications of this examination of intra- and inter-specific variability at crown-level were: (1) the wavelet transform is a robust tool for the identification of tree species using hyperspectral data because it can provide a systematic view of the spectra at multiple scales; and (2) it may be impractical to identify every species using only hyperspectral data, given that spectral similarity may exist between species and that within-crown/species variability may be influenced by many factors.

Keywords: Hyperspectral; Tropical forests; Spectral variation; Derivative; Wavelet; Spectral angle

1. Introduction

Tropical moist and wet forests represent some of the most biologically diverse, structurally complex and carbon-rich ecosystems on Earth. Tropical forests have the intrinsic property of being extremely rich in terms of number of species and species density (Hubbell, 1979, 1997, 2001; Leigh et al., 2004; Wright, 2002). Uncontrolled deforestation processes currently threaten the large biodiversity resources present in tropical environments. These processes, promoted in many cases by land reclamation policies (Sanchez-Azofeifa et al., 2001), do not take into consideration the environmental services that tropical ecosystems provide (Daily et al., 2001). The identification of tree species is a key element in the definition of habitats of key fauna that use specific trees for food and shelter. Recently the Maquenque National Park was created in Costa Rica to protect *Ara ambigua* (the endangered great green macaw) and *Dipterix panamensis* (a tree species). State of the art monitoring systems aimed at forest tree species identification using airborne and then spaceborne sensors are potentially key tools for the development of sustainable development policies (Sanchez-Azofeifa et al., 2003).

The identification and mapping of forest tree species is conducted relatively reliably either in the field or through the interpretation of large scale (>1:4000) aerial photographs (Gong et al., 2001). However, both methods are costly and time consuming. Remote sensing measurements have the potential to provide a cost effective means to examine the complexity of these forests and to generalize findings from plot scale. Broad band spectral measurements (e.g. 100–200 nm)

* Corresponding author. Tel.: +1 780 492 0345; fax: +1 780 492 2030.
E-mail address: benoit.rivard@ualberta.ca (B. Rivard).

0034-4257/$ - see front matter © 2006 Elsevier Inc. All rights reserved.
doi:10.1016/j.rse.2006.06.010

collected by satellite sensors such as SPOT high resolution visible (HRV) and Landsat Thematic Mapper (TM) can be used to distinguish broad groups of communities under different stages of succession (Cochrane, 2000; Foody & Curran, 1994; Kalacska et al., 2004; Roberts et al., 2002; Steininger et al., 2001), but lack the capability to perform identification of individual species (Achard et al., 2002; Foody et al., 2003; Powell et al., 2004).

Airborne hyperspectral remote sensing technology, with its inherent high spectral resolving properties, has been applied in a variety of research fields in forestry such as forest biochemistry (e.g. Curran, 1989; Grossman et al., 1996; Jacquemoud et al., 1996; Johnson & Billow, 1996; Kokaly & Clark, 1999; Martin & Aber, 1997; Peterson et al., 1988; Wessman et al., 1989; Zagolski et al., 1996) and leaf area and stand structure characterization (e.g. Gong et al., 1992). Although the use of hyperspectral data for tree species recognition has been explored (Cochrane, 2000; Fung et al., 1999; Gong et al., 1997, 2001; Martin et al., 1998) with accuracies of up to 91% for sun-lit tree crowns (Gong et al., 2001), most tropical forest studies were based on spectra of leaves or branches alone; studies of whole canopies have been mainly confined to conifer forests. For example, Cochrane (2000) demonstrated the potential for separation of different tropical species based on the foliage reflectance (450–950 nm) of 11 species in southern Pará, Brazil. Fung et al. (1999) used laboratory-derived hyperspectral data (400–900 nm) and a linear discriminant classifier to discriminate 12 subtropical tree species with an accuracy of 84%. More importantly, little research to date has been conducted on the identification of tropical tree species at the crown level using airborne hyperspectral imagery, a problem that is compounded by the strong control of canopy structure in addition to leaf-level spectral reflectance on canopy level information (Asner, 1998). To the best of our knowledge, the work by Clark et al. (2005) is the only one that explores the potential of airborne hyperspectral data for mapping tree species of tropical forests.

Multiple factors can introduce spectral variance within tree crowns or species: reflectance, absorption, and transmission properties of leaves and wood, viewing geometry and a host of other environmental factors such as microclimates, soil characteristics, precipitation, topography and soil moisture (Portigal et al., 1997). In addition, foliage age (Gausman, 1985; Roberts et al., 1998), position in the canopy (Danson, 1995), chlorophyll content (Zarco-Tejada et al., 2003), forest vigor (Luther & Carroll, 1999) and the presence of lianas (Castro-Esau et al., 2004) have been shown to cause substantial variation in the spectral response of some species at the leaf level. Whether or not species identification is possible at the crown level using multi or hyperspectral remote sensing data is determined by: (1) variation within individual tree crowns; (2) variation between tree crowns of the same species; and (3) variation between spectra of different species. An efficient methodology for the discrimination of tree species at the crown level hinges on significantly smaller spectral variation within and amongst tree crowns of the same species than that amongst different species.

The spectral separability of vegetation presents challenges because the number of independent variables that influence the spectra is small (Price, 1992, 1994). The reflectance of vegetation from different species is therefore similar (Portigal et al., 1997). Derivative analysis is a common tool used to suppress the effects of background and brightness differences and enhance subtle spectral difference amongst spectra (Bubier et al., 1997; Gong et al., 1997; Martin & Aber, 1997; Martin et al., 1998; Niemann, 1995; Shaw et al., 1998; Fung et al., 1999). The benefit of derivative spectra has been reported in the identification of tree species predominantly from laboratory investigations at the leaf level or based on *in situ* spectral measurements over tree crowns (Castro-Esau et al., 2004; Cochrane, 2000; Gong et al., 1997; Van Aardt & Wynne, 2001). It remains unclear whether derivative spectra can be used to facilitate the separation of canopy tree species using airborne hyperspectral data, given that airborne hyperspectral data may have a much lower signal-to-noise ratio (SNR) than laboratory or *in-situ* spectral measurements. Recently, wavelet transforms have been introduced for the analysis of hyperspectral data as an efficient means of feature extraction at multiple scales. Case studies on the use of wavelet transforms for a variety of purposes, including automatic detection of subpixel hyperspectral targets (Bruce et al., 2001), pixel unmixing (Li, 2004), automatic dimension reduction of hyperspectral data (Kaewpijit et al., 2003), forest canopy structure identification (Bradshaw & Spies, 1992), weed detection (Koger et al., 2003), and evaluation of the impact of crop residue on the hyperspectral reflectance of soybean and weeds (Huang et al., 2001) have been reported in the literature.

The objective of this paper is to investigate the potential of derivative and wavelet analysis for tree species discrimination at the canopy scale using airborne hyperspectral data of a tropical lowland wet forest. We examine how these transforms impact the spectral variation within given crowns and species and between a selected number of tree species that are not contaminated by the presence of liana or epiphytes. Airborne HYperspectral Digital Collection Experiment (HYDICE) data collected over the La Selva biological station (LS), Costa Rica, is analyzed over 17 tree crowns of 5 species identified in the field. The measure of spectral angle (Clark et al., 2005; Cochrane, 2000; Kruse et al., 1993) is used to quantify the spectral variation observed within or between crowns and species because of its sensitivity to spectral shape. This study complements a recent investigation of this airborne data by Clark et al. (2005) who obtained an overall classification accuracy of 92% for 7 species (including one in this study) using 30 reflectance bands optimally-selected by linear discriminant analysis.

2. Study site and data

2.1. Study site

We conducted the study at the La Selva Biological Station, located near the Sarapiquí River in northeast Costa Rica. This forest is primarily a mixture of lowland primary and secondary

tropical wet forest (Holdridge et al., 1971). The elevation range at La Selva is between 35 and 135 m above sea level. The soils in the region are primarily a mixture of Inceptisols (particularly in alluvial terraces) in the north and residual Ultisols to the south (Clark et al., 1998).

Five tree species common to the region were selected for the study (Table 1). Multiple crowns for each species were identified in the field by expert taxonomists and selected based on their unambiguous location in the imagery (Fig. 1), their large size, and their apparent lack of lianas and epiphytes masking the tree foliage. One crown of *T. oblonga* (TO-1 in Table 1) harbors abundant epiphytes (mostly bromeliads) but was included to investigate the impact of epiphytes on the spectral response of the host tree species.

2.2. Airborne HYDICE hyperspectral data

Airborne HYDICE hyperspectral images provided by the Organization for Tropical Studies (OTS) were used for this study. The HYDICE sensor collects upwelling radiance data in 210 optical bands with a nominal full width at half maximum (FWHM) of 10 nm covering a spectral range of 400–2500 nm (Basedow et al., 1995). HYDICE data were acquired under a clear sky at 13:54 UTC, March 30th, 1998. The selected flight line for this study covers a ground area of 486.4 m wide by 1459.2 m in length and image pixels have an approximate spatial dimension of 1.6 m×1.6 m allowing individual tree crowns to be resolved (Fig. 1). Our analysis and discussion focuses on the visible (440–700 nm) and near infrared (700–1000 nm) spectrum because this spectral region contains information relevant to the biochemistry and structure of vegetation (Blackburn, 1998, 1999; Carter, 1998; Elvidge & Chen, 1995; Schepers et al., 1996; Thenkabail, 2002; Thenkabail et al., 2000, 2002, 2004), and past research has outlined the importance of this wavelength region for species discrimination (Cochrane, 2000; Fung et al., 1999; Gong et al., 1997; Martin et al., 1998). Although the short wave infrared spectral region is reported to be important for the discrimination of tree species (Asner, 1998; Clark et al., 2005; Roberts et al., 2004), it was not included in this study because the data has a low signal-to-noise ratio (Nischan et al., 1999).

Table 1
Species and tree crowns used in the study

Species (family)	Tree crown label ID	No. of HYDICE pixels
Castilla elastica (Moraceae)	CE-1	31
	CE-2	22
Ficus insipida (Moraceae)	FI-1	65
	FI-2	46
	FI-3	47
	FI-4	40
	FI-5	36
	FI-6	41
Luehea seemannii (Tiliaceae)	LS-1	20
	LS-2	22
Terminalia oblonga (Combretaceae)	TO-1[a]	77
	TO-2	56
	TO-3	26
	TO-4	32
Zygia longifolia (Fabaceae)	ZL-2	66
	ZL-3	60
	ZL-4	25

[a] Tree crown hosting numerous epiphytes.

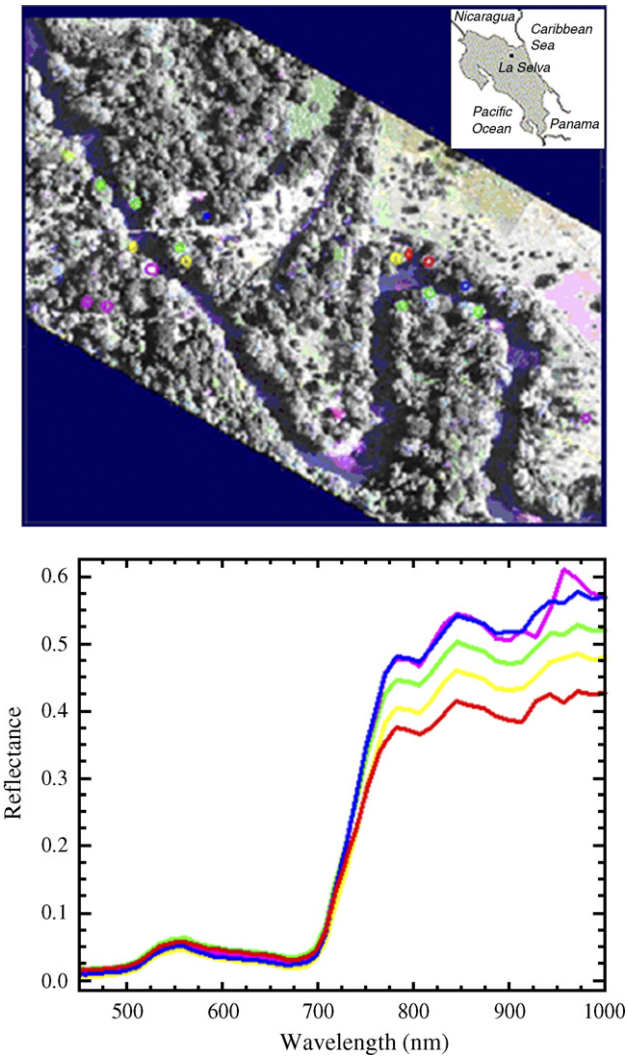

Fig. 1. Color composite of HYDICE bands (red=641 nm, green=552 nm, blue=460 nm) showing the location of the 17 tree crowns sampled. The bottom figure shows the average reflectance spectrum of each species. Crown colors are for the following species: green=*F. insipida*, yellow=*Z. longifolia*, red=*C. elastica*, blue=*L. seemannii*, magenta=*T. oblonga*.

HYDICE-derived radiance values were converted to surface reflectance using the ACORN v4.0 atmospheric correction (Analytical Imaging and Geophysics LLC, Boulder, Colorado) and a tropical atmospheric mode with an atmospheric visibility of 100 km. Atmospheric water vapor was automatically estimated on a per-pixel basis using the water absorption at 940 nm (ACORN 4.0 User's Guide, Analytical Imaging and Geophysics LLC, Boulder, Colorado; Gao et al., 1993). To assess the atmospheric correction and to adjust the wavelength calibration, we used field reflectance spectra acquired in 2002 with an ASD FieldSpec spectrometer (Analytical Spectral Devices, Boulder, CO) over a roof-top easily identified within the HYDICE scene. Fig. 2 shows the calibrated HYDICE

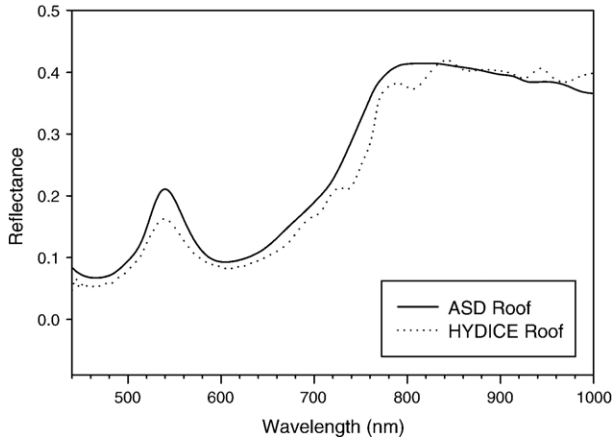

Fig. 2. Mean reflectance spectra from calibrated HYDICE data and field ASD measurement for a green roof-top. The ASD spectrum has been convolved to the HYDICE wavelength profile. The mean HYDICE spectrum is for 5 pixels while the mean ASD measurement is for 3 spectra for different location on the roof. Generally two spectra are similar in the shape. Residual features possibly associated with water are visible near 730 nm, 820 nm, 910 nm on the calibrated HYDICE spectrum, which may result from the combination of poor radiometric calibration, sensor noise, error in water vapor estimates and the difference in time between HYDICE and field measurements.

reflectance and field-measured ASD reflectance for the roof-top. The HYDICE spectrum is similar to the field spectrum but residual absorption features are visible around 730 nm, 820 nm, 910 nm and 950 nm in the calibrated HYDICE spectrum. These may result from the combination of errors in the radiometric calibration, sensor noise, errors in water vapor estimates and the 4 years separating the collection of the HYDICE and field measurements.

To minimize the impact of variable illumination on crown spectra, our analysis is restricted to sun-lit pixels of each tree crown. Sun-lit pixels were manually selected based on the true color composite. The average reflectance spectrum of each species (Fig. 1) illustrates their spectral similarity. The TO-1 crown, because of its epiphytic coverage, was excluded when calculating average spectrum for *T. oblonga*.

3. Methodology

3.1. Derivative spectra

Derivatives of spectra are commonly employed in hyperspectral investigations of vegetation (Castro-Esau et al., 2004; Cochrane, 2000; Gong et al., 1997; Van Aardt & Wynne, 2001). Derivatives are relatively less sensitive to variations in illumination intensity caused by cloud cover and topography (Tsai & Philpot, 1998), and hence should enhance the spectral contrast between different classes. In this study, we examine whether the first derivative of spectra reduces the variation within and between crowns of a given species and enlarges the differences between tree species. Derivatives are estimated using a "finite difference approximation" (Tsai & Philpot, 1998) following smoothing of the reflectance spectra with a mean filter of three wavebands.

3.2. Wavelet transforms

The wavelet transform is a relatively new signal-processing tool that is used to provide a systematic analysis of signals (e.g. spectra in this study) at various "spectral scales" or different band passes that are determined by the width of the wavelet basis function (Bruce et al., 2001). The wavelet transform decomposes the hyperspectral signal into sets of coefficients, with each set associated with a spectral scale and each element in a set associated with a particular wavelength location. With the continuous wavelet transform (CWT), a spectrum can be decomposed and analyzed across a series of continuous spectral scales (Bruce & Li, 2001). With the discrete wavelet transform (DWT), signals are analyzed over a discrete set of scales, typically being dyadic (2^j, $j=1, 2, 3,\ldots$), and the transform can be realized using a variety of fast algorithms (Bruce et al., 2001). Only the ortho-normal DWT (e.g. HAAR wavelet in this paper) was used in this paper because: (1) the information carried at different scales is orthogonal and non-redundant, e.g. the variance at various scales is separable and the sum of variances at all scales will be equal to the variance in the original signal (Lindsay et al., 1996); (2) the effectiveness of DWT has been reported in the detection and classification of vegetation species (Bruce et al., 2001; Koger et al., 2003; Li, 2004); and (3) the computation of DWT is very fast and the transformed results are easier to manipulate. Further information on the development of DWT can be found in Daubechies (1992) and Mallat (1989).

The fine-scale and coarse-scale information of hyperspectral signals can be simultaneously investigated by projecting the signal onto a set of wavelet bases with different scales, a process referred to as multiresolution analysis of signals (MRA) (Mallat, 1989). Given a mother wavelet $\psi(\lambda)$, the wavelet transform coefficients of the hyperspectral signal $f(\lambda)$ are calculated by the inner product

$$W(s,b) = \langle f(\lambda), \psi_{s,b}(\lambda) \rangle \quad (1)$$

with $W(s,b)$ referring to wavelet transform coefficients of signal $f(\lambda)$ and $\psi_{s,b}(\lambda)$ referring to wavelet bases. The wavelet bases, $\psi_{s,b}(\lambda)$, can be formed from the mother wavelet, $\psi(\lambda)$, by a series of scaling and shifting operations using:

$$\psi_{s,b}(\lambda) = \frac{1}{\sqrt{s}} \psi\left(\frac{\lambda - b}{s}\right) \quad (2)$$

where the variable s indicates the scale (or width) of a particular basis function and the variable b specifies its shifted position.

The discrete wavelet transform (DWT) was implemented using the fast filter tree algorithm developed by Mallat (1989), which is a dyadic (e.g. the resolution is decreased by a factor of two between two scales) discrete implementation of the wavelet transform (Fig. 3). The input to the filter tree, $f(\lambda)$, is the hyperspectral signal (e.g. reflectance spectrum), and the signal is then passed through a series of high-pass and low pass filters (HPF and LPF). After each filter is applied, the signal is degraded by a factor of 2. Supposing the original signal has

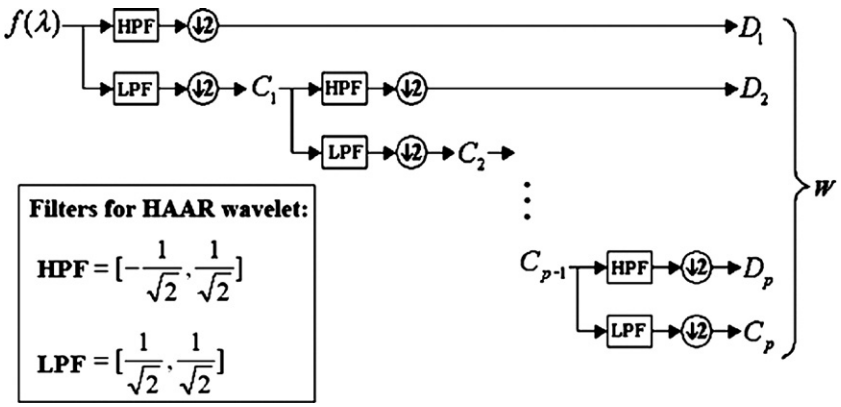

Fig. 3. Illustration of DWT. $f(\lambda)$ is the input hyperspectral signal. Blocks HPF and LPF represent operations of high-pass and low-pass filtering, respectively, which are accomplished by convolving input signal $f(\lambda)$ with appropriate filter kernels. Symbol (↓2) denotes the operation of down sampling, which means the input signal will be decimated by a factor of 2. $\boldsymbol{C}_i$ and $\boldsymbol{D}_i$ are vectors for approximation and detail coefficients at scale i. The insert shows the filters for HAAR wavelet used in this paper.

$N=2^k$ elements, the output from the first filter operation will have only 2^{k-1} elements, and the output from the second filter will have 2^{k-2} elements, and so on. The final stage of the decomposition will yield an output which has only one (2^0) element. The outputs of the high- and low pass filters at scale s are called the wavelet detail and approximation coefficients (D_s and C_s), respectively. At each stage of the filter tree, the wavelet approximation coefficients from the previous scale are used as the input to the next stage.

The final result of the DWT decomposition of a spectrum is a set of wavelet coefficients that are represented as a vector: $\boldsymbol{W}=[\boldsymbol{C}_p,\boldsymbol{D}_p,\ldots,\boldsymbol{D}_2,\boldsymbol{D}_1]$ (p is the coarsest decomposition level). For this vector, each wavelet coefficient is directly related to the amount of energy in the signal at a particular scale. It should be noted that W is dependent on the selection of the mother wavelet function. Pu and Gong (2004) found that the energy feature from a third order mother wavelet of the Daubechies family (db3) is well correlated with LAI. Bruce et al. (2001) found the HAAR wavelet to be 1 of 6 most useful wavelets for target detection following the investigation of 36 commonly used mother wavelets. In this study, the HAAR wavelet was selected because recent investigations (Bruce et al., 2001; Li, 2004; Li et al., 2001) have illustrated its effectiveness for the feature extraction of hyperspectral data.

A variety of parameters can be computed from the DWT decomposition, such as the wavelet coefficients, their energy, and any combination of the two. The most commonly used parameter is the DWT energy feature vector ($\boldsymbol{F}_{\mathrm{E}}$):

$$\boldsymbol{F}_{\mathrm{E}} = D_1^{\mathrm{E}}, D_2^{\mathrm{E}}, \ldots, D_p^{\mathrm{E}}, C_p^{\mathrm{E}}] \tag{3}$$

where $\boldsymbol{F}_{\mathrm{E}}$ is referred to as a wavelet energy feature vector, p is the coarsest scale of the discrete wavelet decomposition. D_j^{E} is the root mean square energy of the wavelet detail coefficient D_j at scale j, computed as,

$$D_j^{\mathrm{E}} = \sqrt{\frac{1}{K_j}\sum_{k=1}^{K_j}[D_j(k)]^2}, \tag{4}$$

where K_j is the number of elements in the wavelet detail coefficient D_j . C_p^{E} is the root mean square energy of wavelet approximation coefficient C_p at the coarsest scale, p, and can be similarly calculated.

While the wavelet energy feature (F_{E}) represents the energy distribution of the original spectrum across different scales, the wavelet detail coefficient (D_j) reveals the spectral information in hyperspectral signals at a specific spectral scale j. Research on sub-pixel target detection and spectral mixture analysis using hyperspectral data have shown a reduction of the within-class variance and an increase of the between-class variance using F_{E} (Bruce et al., 2002) or the wavelet detail coefficient at a specific scale (Li, 2004), which may be valuable for the identification of tree species. In this study, reflectance spectra with 64 bands between 440 and 1000 nm were used as inputs to the DWT, resulting in the maximum decomposition level of 6 (e.g. $2^6=64$).

3.3. Spectral angles for the quantification of spectral variability

The spectral angle between two spectra has been used extensively in the hyperspectral remote sensing community for mineral mapping (Kruse et al., 1993; Price, 1994) and to quantify the similarity between spectra from different tree species (Clark et al., 2005; Cochrane, 2000; Price, 1994). Given that n spectra, $[s_1,s_2,\ldots,s_n]$, are sampled from a single species or crown, and that these spectra provide a mean vector $\bar{\boldsymbol{s}}$, the standard deviation of spectral angles between $s_i (i=1, 2,\ldots,n$ and $\bar{\boldsymbol{s}}$ can be used to estimate the spectral variation within a crown or amongst crowns of a species. A small standard deviation will be indicative of the small spectral variation within the species or crown. In addition, a Kolmogorov–Smirnov test is used to test the normality of the spectral variation within single tree crown and a Kruskal–Wallis test is used to test the equivalence of the medians of spectral angle amongst the crowns of a given species.

In this study we do not use the well-known Jeffries–Matusita distance to measure separability between species because

spectral angle measurements for crowns do not follow a normal distribution (as indicated in Section 4.1). Instead, we use a simple index ($d(i,j)$, Eq. (5)) to indicate the spectral separability between species, taking into account both the inter-species and intra-species variability (Bruce et al., 2002),

$$d(i,j) = (\mu_i - \mu_j)^2 \left(\frac{1}{\sigma_i^2} + \frac{1}{\sigma_j^2} \right) \quad (5)$$

where μ_i and σ_j are the mean value and standard deviation of spectral angles between the reference spectrum (s_{ref}) and each pixel of a species and μ_i and σ_j are values for a different species. A higher inter-species variability and smaller intra-species variability will result in a larger d value. This index is used to study changes in species separability as a function of the spectral transform (e.g. derivative, wavelet). For this purpose and as indicated below the average spectrum of a specific crown (FI-1) was selected as a reference spectrum against which all other spectra were compared.

4. Results

4.1. Reflectance variability within crowns of F. insipida

In this section we examine the reflectance variability within crowns and the variation or similarity amongst crowns of *F. insipida*. Large variations within or between crowns of a given species will decrease the potential for the unique identification of this species. We selected *F. insipida* because it had the largest number of crowns accessible in the field (FI-1, FI-2, FI-3, FI-4, FI-5 and FI-6).

Spectral angles were computed between all pixels belonging to a crown and the mean spectrum of the crown. Histograms and statistics of the spectral angle for each crown (Fig. 4) vary considerably across different tree crowns. The lowest standard deviation (0.019) is observed for FI-3, with a maximum of 0.034 for FI-2. The p values from the Kolmogorov–Smirnov test are 0.006 (FI-1), <0.001 (FI-2), 0.184 (FI-3), >0.200 (FI-4), >0.200 (FI-5) and <0.001 (FI-6). FI-3, FI-4 and FI-5 display a normal distribution of angles, with a confidence level of 95%.

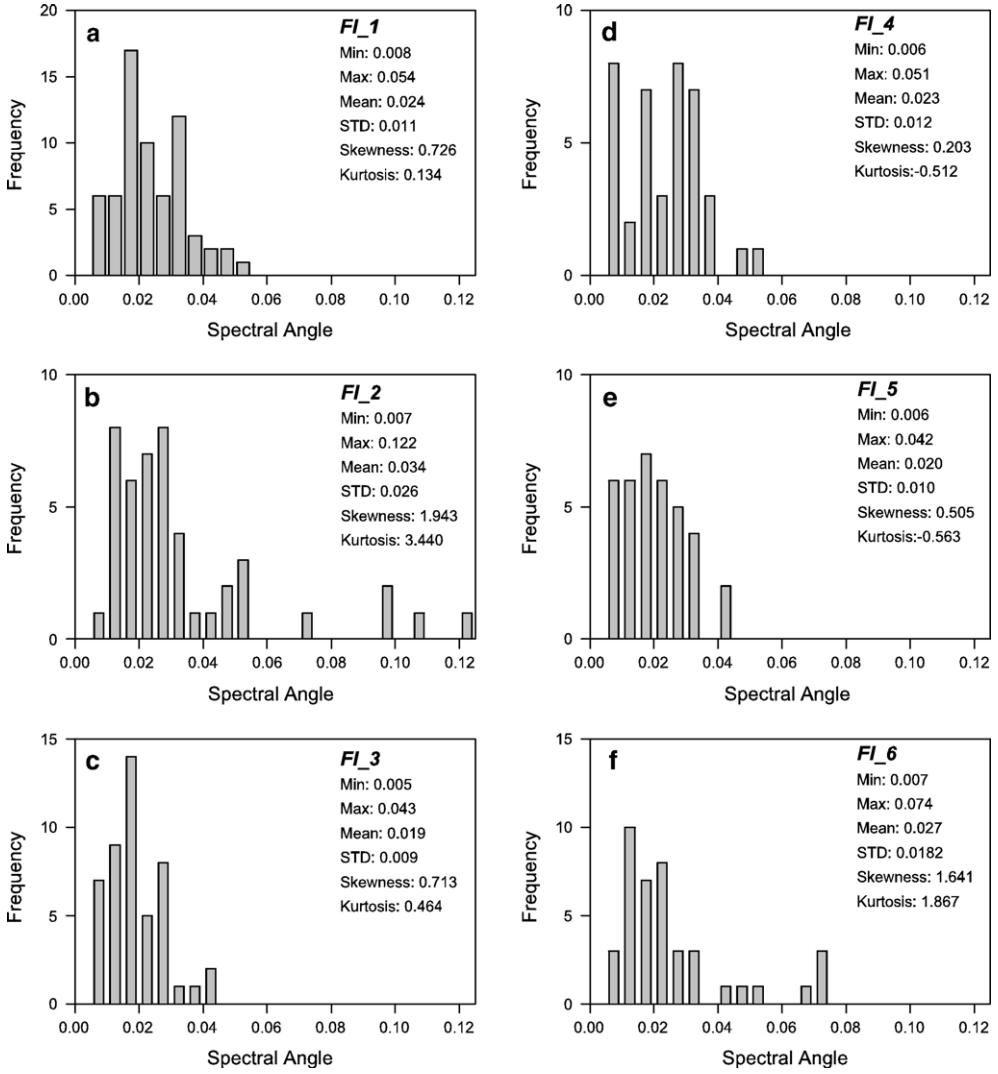

Fig. 4. Histograms of the spectral angle within six crowns of *F. insipida* calculated from the reflectance data (spectral angle in radian).

Since the variance of the spectral angle is not equal for different crowns and the distribution is not always normal, we used a Kruskal–Wallis test, a nonparametric version of the one-way ANOVA, to test whether the medians of spectral angle are different amongst the crowns. The H value for the Kruskal–Wallis test is 13.8, indicating that the null hypothesis of "no difference amongst different crowns" should be rejected at a significance level of 0.05 ($df=5$, right-tail probability $p=0.017$).

4.2. Comparative results for the reflectance, derivative and wavelet domains

The ability of derivatives and wavelets to suppress within-crown variations of *F. insipida* was examined (Fig. 5 and Table 2). The detail coefficients resulting from the discrete HAAR wavelet transform at fine scales are equivalent to a first order approximation of the first derivative spectrum, thus the results from the detailed wavelet coefficients at scales 1 and 2 are not listed in Fig. 5 and Table 2. The maximum decomposition level, scale 6, was not included in the analysis since the detail coefficient at this scale consists of only one element ($2^0=1$) (Section 3.2).

The range of spectral angle and standard deviation within individual tree crowns is much larger for first derivatives as opposed to wavelet and reflectance domains (Fig. 5 and Table 2). In the wavelet domain, spectral variation is greatly reduced for all crowns at scale 5 and for the wavelet energy feature. At wavelet scale 3, the spectral variation is larger than that of the reflectance domain. At scale 4, all crowns except FI-6 display a standard deviation of spectral angle similar to that of the reflectance domain (Table 2). Although derivative spectra have been used extensively for hyperspectral investigations of vegetation, their use is less than optimal for the identification of tree species (e.g. *F. insipida*) at the crown level. In contrast, wavelet scale 5 and the wavelet energy feature appear considerably more useful for the identification of tree species (e.g. *F. insipida*).

Table 2
Standard deviation of the spectral angle within crowns of *F. insipida* in the reflectance, first derivative and wavelet domains

	FI-1	FI-2	FI-3	FI-4	FI-5	FI-6
Reflectance	0.011	0.026	0.009	0.012	0.010	0.018
First derivative	0.025	0.039	0.020	0.029	0.026	0.022
WL-Scl3	0.018	0.027	0.015	0.014	0.024	0.017
WL-Scl4	0.014	0.024	0.013	0.010	0.013	0.009
WL-Scl5	0.003	0.008	0.002	0.004	0.003	0.004
WL-energy	0.006	0.015	0.005	0.008	0.007	0.008

4.3. Spectral variability of other species

Following the analysis for *F. insipida*, the spectral angle distribution was computed for the remaining species by comparing each pixel in a species to the mean spectrum of the same species (Fig. 6). Results from the derivative domain were excluded from the analysis based on the finding for *F. insipida*. As observed for *F. insipida*, the spectral variation

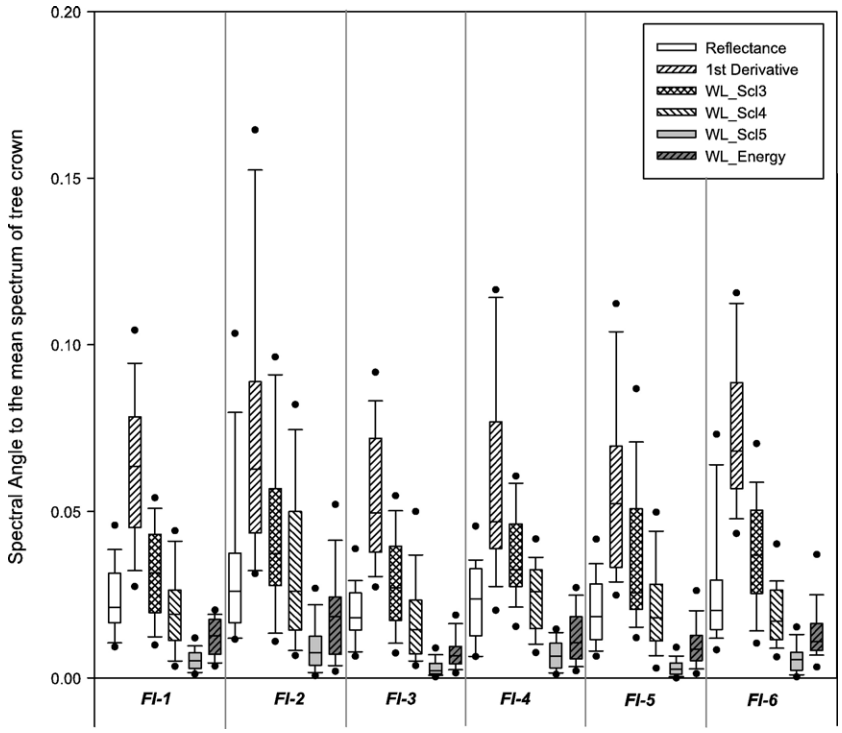

Fig. 5. The distribution of spectral angle within six crowns of *F. insipida* calculated from the reflectance, first derivative, and wavelet domains. The boundaries of the box indicate the 25th and 75th percentiles, a line within the box marks the median, whiskers above and below the box indicate the 90th and 10th percentiles, and dots represent the 5th and 95th percentiles.

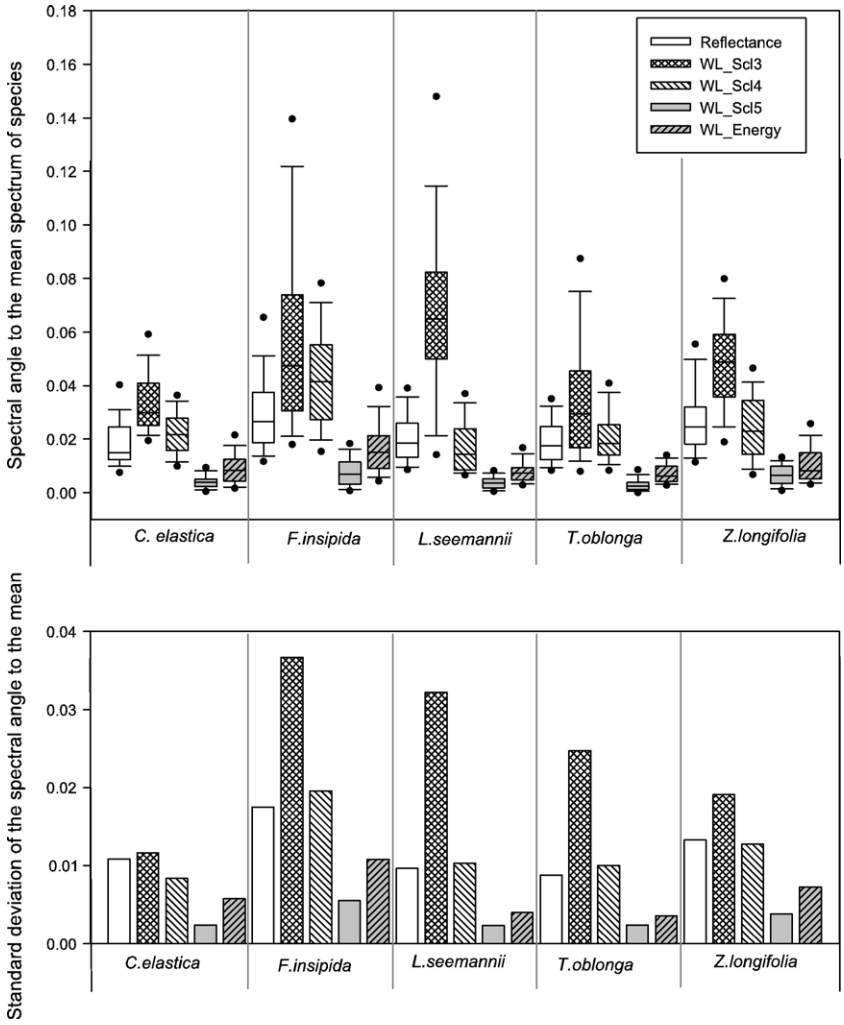

Fig. 6. The distribution of spectral angle within each species (crown 1 of *T. oblonga* (TO-1) was excluded from the analysis due to the presence of epiphytes). Top: variation from the mean spectrum. The boundaries of the box indicate the 25th and 75th percentiles, a line within the box marks the median, whiskers above and below the box indicate the 90th and 10th percentiles, dots represent the 5th and 95th percentiles; bottom: standard deviation of the spectral angle.

within the remaining species is greatly reduced for the detail coefficient of scale 5 and for the wavelet energy feature.

4.4. Spectral separability of tree species

As shown above, the wavelet coefficients at coarse scales and the wavelet energy feature can suppress the spectral variation within individual crowns or within species and thus should enhance the spectral separability of species (Eq. (5)). To examine spectral discrimination of the different species, the spectral angle of each pixel from the mean spectrum of *F. insipida* crown #1 (FI-1) was determined. The mean and standard deviation for each species were calculated and the spectral separability was obtained using Eq. (5). It should be noted that selecting a reference spectrum other than FI-1 would have resulted in different angles.

Table 3 lists the separability for the 5 species using data in the reflectance and wavelet domains. The worst separability value approaches 0 and is observed for *F. insipida* and *C. elastica*, while *T. oblonga* displays the largest separability from *F. insipida* and *C. elastica*. The best separability results are at the wavelet scale 5 or the energy feature with one exception (CE vs. ZL at scale 4) while the worst separability is consistently observed at wavelet scale 3.

Table 3
Spectral separability (e.g. $d(i,j)$ values calculated from Eq. (5)) between species using data from the reflectance and wavelet domains[a]

	Reflectance	WL-Scl3	WL-Scl4	WL-Scl5	WL-energy
CE vs. FI	0.051	0.020	0.525	0.038	0.670
CE vs. LS	15.891	14.087	32.352	41.140	17.22
CE vs. TO	60.223	39.171	86.074	105.334	101.181
CE vs. ZL	23.557	20.179	41.013	22.939	23.007
FI vs. LS	9.260	8.169	12.647	27.165	23.444
FI vs. TO	42.626	25.365	37.682	74.763	115.669
FI vs. ZL	13.751	10.885	15.079	12.178	25.986
LS vs. TO	15.069	2.053	12.695	10.952	33.505
LS vs. ZL	2.814	0.110	1.162	0.291	3.749
TO vs. ZL	2.321	1.144	4.857	11.630	7.445

[a] The highest and lowest separability values for each species pair are highlighted. TO-1 is omitted.

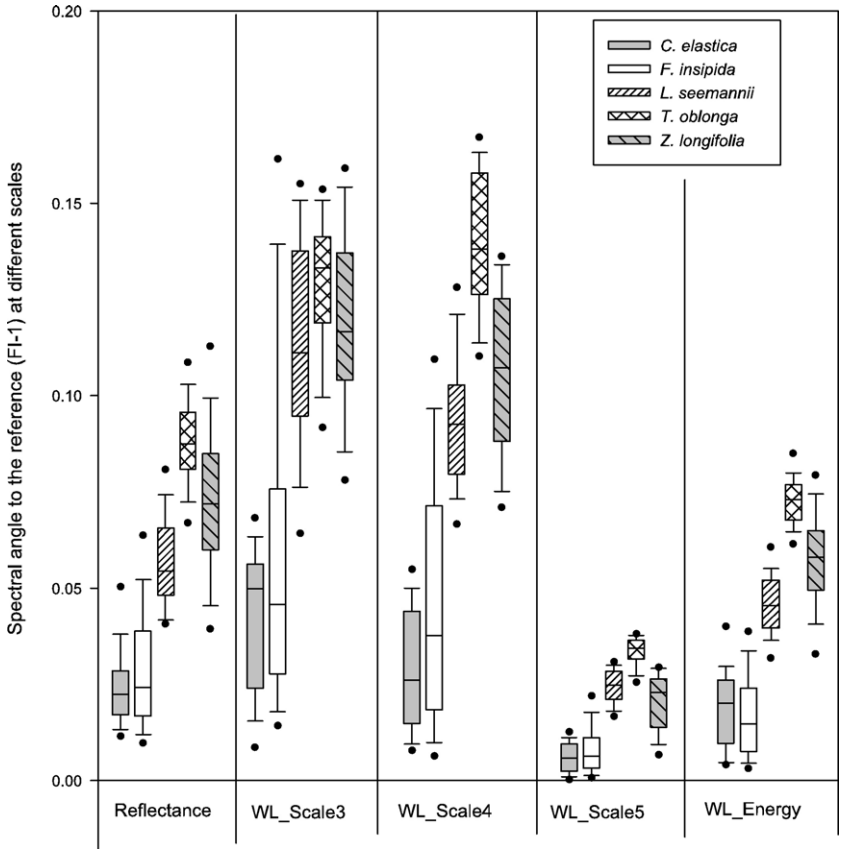

Fig. 7. The distribution of spectral angle of each species with respect to FI-1. The boundaries of the box indicate the 25th and 75th percentiles, a line within the box marks the median, whiskers above and below the box indicate the 90th and 10th percentiles, and dots represent the 5th and 95th percentiles.

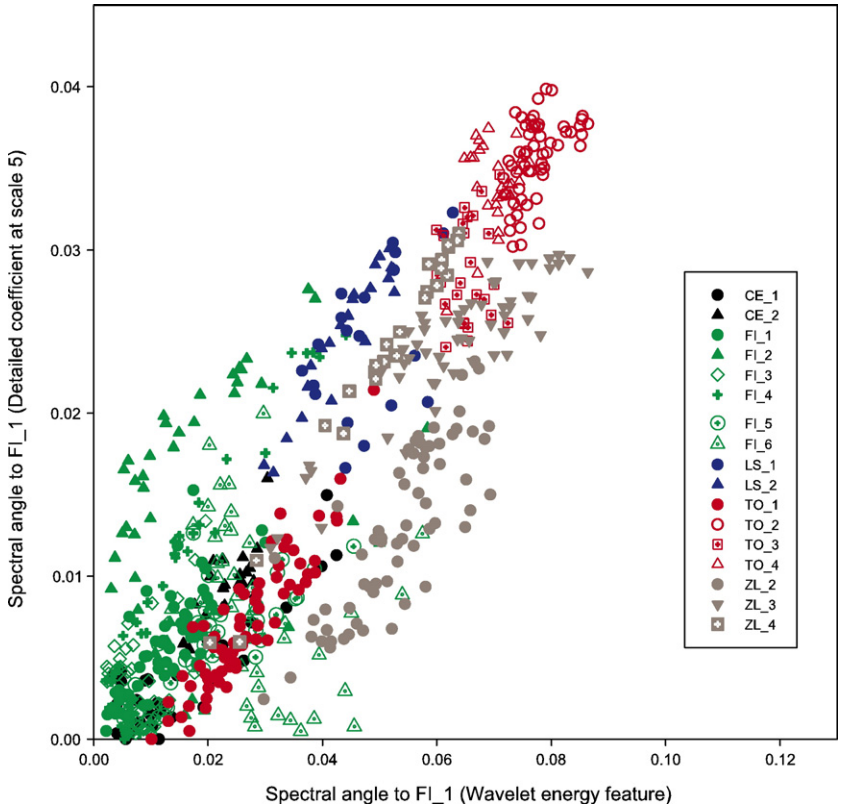

Fig. 8. Scatter plot of energy feature and coefficients values at wavelet scale 5.

Fig. 7 provides an additional representation of the spectral separability of species. The distribution of spectral angle for CE and FI consistently overlap explaining the near zero separability seen in Table 3. *L. seemannii*, *T. oblonga* and *Z. longifolia* are not clearly distinguished in the reflectance domain, though each species displays a different distribution of angles. The large intra-species variation and large overlap of spectral angle distribution observed for these species at scale 3 explains their lowest separability at this scale (Table 3). The separability of *Z. longifolia* and *C. elastica* improves at scale 4 compared to the reflectance domain, but the same is not true of other species due to their larger intra-species variability at scale 4. Intra-species variability is considerably smaller at wavelet scale 5 and for the energy feature, in part explaining the larger separability values obtained at these two scales (Table 3). *T. oblonga* can be separated well from *Z. longifolia* at scale 5. *Z. longifolia*, *L. seemannii* and *T. oblonga* are clearly discriminated from *F. insipida* and *C. elastica* using the wavelet energy feature. *L. seemannii*, though not quite distinguishable from *Z. longifolia* using the wavelet energy feature, is not confused with *T. oblonga*.

4.5. Visualization of the separability of different species/crowns

To complement the crown and species scale overview statistics shown above, a scatter plot of spectral angle at scale 5 and wavelet energy feature is shown in Fig. 8 for all pixels of the study. The distinctions observed at the species level are apparent with *T. oblonga* showing distinct values at the upper end, with the exception of crown # 1 (TO-1) that contains an extensive cover of epiphytes. All pixels of TO-1 are displaced to very low values resulting in a complete confusion with *F. insipida* and *C. elastica*. *L. seemannii* and *Z. longifolia* both display intermediate values but each species generally occupies a distinct field in Fig. 8. Note that for these three species, a number of crowns occupy distinct portions of the graph with little overlap from other crowns (e.g. ZL-2, 3, 4).

5. Discussion and summary

The classification of tree species using remote sensing data with high spectral and spatial resolution is mostly controlled by the spectral variation within tree crown/species (intra-species) and the spectral variation between species (inter-species). Knowledge of intra-species variation and inter-species variation is relevant to the accuracy of the final identification results. This study suggests that the spectral intra-crown variation can vary from crown to crown within a given species (e.g. *F. insipida*, Fig. 4) and does not always follow a normal distribution. This result implies challenges to statistically define the spectral variation within species using conventional classification approaches that assume normal distributions. In the research on the discrimination of lianas and tropical forests using leaf-scale hyperspectral data, Castro-Esau et al. (2004) found that nonparametric classifiers performed better than parametric classifiers because nonparametric methods do not require the assumption of normality and have low training error. Our finding that the spectral variation may lack normality at the tree crown level also suggests that nonparametric approaches should be favored for the identification of different tree species in tropical forests.

Although the derivative of reflectance spectra has been used extensively to suppress background signals and enhance subtle spectral features in hyperspectral remote sensing of vegetation, our results suggest that it may not be optimal for species identification in tropical forests using airborne hyperspectral data because it does not effectively suppress the spectral variation within tree crowns or species. Fung et al. (1999) also found poorer results from derivative spectra than from the original reflectance in the discrimination of subtropical tree species. The derivative is very sensitive to noise in the original spectrum. Smoothing prior to derivative calculation can only remove part of the noise. The residual noise will be emphasized in the derivative spectra and this may vary according to the pixel location on the tree crown. In addition, environmental or stress factors such as moisture content and leaf age introduce subtle variations in crown reflectance that will be enhanced by the differentiation. Consequently, spectral variation within crowns or species will be greatly enlarged in the derivative spectral domain, further interfering with the identification of tree species. In this study, the spectral variation of *F. insipida* was almost twice as large using first derivative spectra as compared to reflectance spectra (Fig. 5).

Our results suggest that the DWT wavelet transform can be a very useful tool for species identification. The wavelet coefficients at coarse scales and the wavelet energy feature are capable of reducing the variation of samples within crowns/species and capturing the spectral differences between species. The maximum separability amongst five species was reached using either the wavelet energy feature or wavelet coefficients at scales 4 and 5 (Table 3). In contrast, wavelet coefficients at fine scales may not be informative for the purpose of identification of tree species. At fine scales, wavelet coefficients are sensitive to narrow or local spectral features because they are derived from high-pass filters, which is similar to the derivative spectra. The wavelet coefficients at coarse scales and the wavelet energy feature are mainly controlled by the broad spectral pattern of the spectrum (Kempeneers et al., 2005), thus a more global view of reflectance may be more useful for the identification of tree species at the crown level than simply observing the reflectance at finely resolved spectral bands.

Koger et al. (2003) also found that coarse scale wavelet coefficients were important in weed detection using hyperspectral data. While this study confirmed that the wavelet energy feature is robust to increase class separability (Bruce et al., 2001, 2002; Huang et al., 2001; Li et al., 2001), we also found the information at coarse wavelet scales to be equally important for species identification (Figs. 7 and 8 and Table 3), though the specific wavelet features and scale may vary for different species. For example, maximum separability between CE and ZL was reached at scale 4 while other species exhibit their greatest separability with the scale 5 wavelet feature or the energy feature (Table 3).

Given that spectral similarity may exist between species and that the within-crown/species variability may be influenced by

many factors, it may be impractical to identify a large number of species using only hyperspectral data. Distinguishing some forest taxonomic groups or species should be feasible, however. For example, clusters of *T. oblonga*, *Z. longifolia* and *L. seemannii* are well separated in Fig. 8; however, *F. insipida* and *C. elastica* are not separable. In addition, in many cases a thorough understanding of tree phenology (e.g. flower production) may be more relevant to the broad detection of populations than the use of complex airborne hyperspectral missions or data analysis approaches. The incorporation of ancillary information such as chlorophyll concentration and leaf area index may be necessary to achieve high levels of accuracy. If combined with LIDAR, which can provide information on tree location and height as well as crown diameter and shape, the accuracy of species classification may be expected to improve further (Gillespie et al., 2004).

Furthermore, leaf optical properties also vary due to many different factors ranging from leaf age, non-sequential leaf flushing, to colonization by epiphytes and galls that cover mature leaf surfaces and reduce light transmission and limit photosynthesis (Coley & Kursar, 1996; Roberts et al., 1998), factors that in turn contribute to differences in spectral reflectance at the crown level for individuals of the same species. This is better explained by considering the effect of epiphytes on crown TO-1. Crown TO-1 in Fig. 8 has a distinct distribution pattern from other TO crowns, demonstrating that structurally-parasitic plants can significantly change the separability between species. Similar results have been observed for canopy trees infested with lianas in a tropical dry forest of Panama (Sanchez-Azofeifa & Castro-Esau, submitted for publication). Differences in chlorophyll concentration and internal leaf structure between epiphytes, lianas and the host canopy may provide only part of the answer as to why epiphytes/lianas can significantly change the spectral behavior of the host canopy (Danson, 1995). Moreover, abundant epiphytes/lianas on the canopy will change the canopy structure (Stuntz et al., 2002), in turn impacting the reflectance at the canopy scale. The results of this study are encouraging for the identification of tropical forest species using hyperspectral data. Further research should aim to enlarge the sample size of epiphyte bearing crown and examine spectral variation observed between shaded and sun-lit portions of crowns.

Acknowledgements

Support was provided by the Inter-American Institute for Global Change Research, the Canada Foundation for Innovation, the Tinker Foundation, the National Science and Engineering Research Council of Canada and the Organization for Tropical Studies (OTS).

References

Achard, F., Eva, H. D., Stibig, H. J., Mayaux, P., Gallego, J., Richards, T., et al. (2002). Determination of deforestation rates of the world's humid tropical forests. *Science*, *297*(5583), 999−1002.

Asner, G. P. (1998). Biophysical and biochemical sources of variability in canopy reflectance. *Remote Sensing of Environment*, *64*, 234−253.

Basedow, R. W., Carmer, D. C., & Anderson, M. E. (1995, Feb. 17–24). HYDICE system: Implementation and performance. *SPIE Proceedings*, *Vol. 2480*. Orlando, FL, USA.

Blackburn, G. A. (1998). Spectral indices for estimating photosynthetic pigment concentrations: A test using senescent tree leaves. *International Journal of Remote Sensing*, *19*(4), 657−675.

Blackburn, G. A. (1999). Towards the remote sensing of matorral vegetation physiology: Relationships between spectral reflectance, pigment, and biophysical characteristics of semiarid bushland canopies. *Remote Sensing of Environment*, *70*, 278−292.

Bradshaw, G. A., & Spies, T. A. (1992). Characterizing canopy gap structure in forests using wavelet analysis. *Journal of Ecology*, *80*, 205−215.

Bruce, L. M., & Li, J. (2001). Wavelets for computationally efficient hyperspectral derivative analysis. *IEEE Transactions on Geoscience and Remote Sensing*, *39*, 1540−1546.

Bruce, L. M., Li, J., & Huang, Y. (2002). Automated detection of subpixel hyperspectral targets with adaptive multichannel discrete wavelet transform. *IEEE Transactions on Geoscience and Remote Sensing*, *40*, 977−980.

Bruce, L. M., Morgan, C., & Larsen, S. (2001). Automated detection of subpixel targets with continuous and discrete wavelet transforms. *IEEE Transactions on Geoscience and Remote Sensing*, *39*(10), 2217−2226.

Bubier, J. L., Rock, B. N., & Crill, P. M. (1997). Spectral reflectance measurements of boreal wetland and forest mosses. *Journal of Geophysical Research - Atmospheres*, *102*(D24), 29483−29494.

Carter, G. A. (1998). Reflectance bands and indices for remote estimation of photosynthesis and stomatal conductance in pine canopies. *Remote Sensing of Environment*, *63*, 61−72.

Castro-Esau, K. L., Sanchez-Azofeifa, G. A., & Caelli, T. (2004). Discrimination of lianas and trees with leaf-level hyperspectral data. *Remote Sensing of Environment*, *90*, 353−372.

Clark, D. B., Clark, D. A., & Read, J. M. (1998). Edaphic variation and the mesoscale distribution of tree species in a neotropical rain forest. *Journal of Ecology*, *86*(1), 101−112.

Clark, M. L., Roberts, D. A., & Clark, D. B. (2005). Hyperspectral discrimination of tropical rain forest tree species at leaf to crown scales. *Remote Sensing of Environment*, *96*, 375−398.

Cochrane, M. A. (2000). Using vegetation reflectance variability for species level classification of hyperspectral data. *International Journal of Remote Sensing*, *21*(10), 2075−2087.

Coley, P. D., & Kursar, T. A. (1996). Causes and consequences of epiphyll colonization. In S. Mulkey, R. Chazdon, & A. Smith (Eds.), *Tropical forest plant physiology* (pp. 337−362). New York: Chapman Hall.

Curran, P. J. (1989). Remote sensing of foliar chemistry. *Remote Sensing of Environment*, *30*, 271−278.

Daily, G. C., Ehrlich, P. R., & Sanchez-Azofeifa, G. A. (2001). Countryside biogeography: Utilization of human-dominated habitats by the avifauna of southern Costa Rica. *Ecological Applications*, *11*, 1−13.

Danson, F. M. (1995). Developments in the remote sensing of forest canopy structure. In F. M. Danson, & S. E. Plummer (Eds.), *Advances in environmental remote sensing* (pp. 53−69). Chichester, UK: Wiley.

Daubechies, I. (1992). *Ten lectures on wavelets.* Philadelphia PA: Society for Industrial and Applied Mathematics.

Elvidge, C. D., & Chen, Z. (1995). Comparison of broadband and narrow-band red and near-infrared vegetation indices. *Remote Sensing of Environment*, *54*, 38−48.

Foody, G. M., Boyd, D. S., & Cutler, M. E. J. (2003). Predictive relations of tropical forest biomass from Landsat TM data and their transferability between regions. *Remote Sensing of Environment*, *85*(4), 463−474.

Foody, G. M., & Curran, P. J. (1994). Estimation of tropical forest extent and regenerative stages using remote sensing data. *Journal of Biogeography*, *21*, 223−244.

Fung, T., Ma, F. Y., & Siu, W. L. (1999). Hyperspectral data analysis for subtropical tree species identification. *Proceedings: 1999 ASPRS Annual Conference, Portland Oregon*.

Gao, B., Heidebrecht, K. B., & Goetz, A. F. H. (1993). Derivation of scaled surface reflectances from AVIRIS data. *Remote Sensing of Environment*, *44*, 165−178.

Gausman, H. W. (1985). *Plant leaf optical properties in visible and near-infrared light.* Lubbock, TX: Texas Tech Press.

Gillespie, T. W., Brock, J., & Wright, C. W. (2004). Prospects for quantifying structure, floristic composition and species richness of tropical forests. *International Journal of Remote Sensing*, *25*, 707−715.

Gong, P., Pu, R., & Miller, J. R. (1992). Correlating leaf area index of Ponderosa pine with hyperspectral CASI data. *Canadian Journal of Remote Sensing*, *18*, 275−282.

Gong, P., Pu, R., & Yu, B. (1997). Conifer species recognition: Exploratory analysis of *in situ* hyperspectral data. *Remote Sensing of Environment*, *62*, 189−200.

Gong, P., Pu, R., & Yu, B. (2001). Conifer species recognition: Effects of data transformation and band width. *International Journal of Remote Sensing*, *22*, 3471−3481.

Grossman, Y. L., Ustin, S. L., Jacquemoud, S., Sanderson, E., Schmuck, G., & Verdebout, J. (1996). Critique of stepwise multiple linear regression for the extraction of leaf biochemistry information from leaf reflectance data. *Remote Sensing of Environment*, *56*, 182−193.

Holdridge, L. R., Grenke, W. C., Hatheway, W. H., Liang, T., & Tosi, J. A., Jr. (1971). *Forest environments in tropical life zones: A pilot study.* Oxford: Pergamon.

Huang, Y., Bruce, L. M., Koger, T., & Shaw, D. (2001). Analysis of the effects of cover crop residue on hyperspectral reflectance discrimination of soybean and weeds via Haar transform. *Proc. IEEE IGARSS*, *Vol. 3* (pp. 1276−1278).

Hubbell, S. P. (1979). Tree dispersion, abundance and diversity in a tropical dry forest. *Science*, *203*, 1299−1309.

Hubbell, S. P. (1997). A unified theory of biogeography and relative species abundance and its application to tropical rain forests and coral reefs. *Coral Reefs*, *16*, S9−S21 (suppl).

Hubbell, S. P. (2001). *The unified neutral theory of biodiversity and biogeography.* Princeton, NJ: Princeton University Press.

Jacquemoud, S., Ustin, S. L., Verdebout, J., Schmuck, G., Andreoli, G., & Hosgood, B. (1996). Estimating leaf biochemistry using the PROSPECT leaf optical properties model. *Remote Sensing of Environment*, *56*, 194−202.

Johnson, L. F., & Billow, C. R. (1996). Spectrometric estimation of total nitrogen concentration in Douglas-fir foliage. *International Journal of Remote Sensing*, *17*, 489−500.

Kaewpijit, S., Moigne, J. L., & El-Ghazawi, T. (2003). Automatic reduction of hyperspectral imagery using wavelet spectral analysis. *IEEE Transactions on Geoscience and Remote Sensing*, *41*(4), 863−871.

Kalacska, M., Sanchez-Azofeifa, G. A., Calvo, J., Rivard, B., Quesada, M., & Janzen, D. (2004). Species composition, similarity and diversity in three successional stages of a tropical dry forest. *Forest Ecology and Management*, *200*, 227−247.

Kempeneers, P., Backer, S. D., Debruyn, W., Coppin, P., & Scheunders, P. (2005). Generic wavelet-based hyperspectral classification applied to vegetation stress detection. *IEEE Transactions on Geoscience and Remote Sensing*, *43*, 610−614.

Koger, C. H., Bruce, L. M., Shaw, D. R., & Reddy, K. N. (2003). Wavelet analysis of hyperspectral reflectance data for detecting pitted morning glory (*Ipomoea lacunosa*) in soybean (*Glycine max*). *Remote Sensing of Environment*, *86*, 108−119.

Kokaly, R. F., & Clark, R. N. (1999). Spectroscopic determination of leaf biochemistry using band-depth analysis of absorption features and stepwise linear regression. *Remote Sensing of Environment*, *67*, 267−287.

Kruse, F. A., Lefkoff, A. B., Boardman, J. W., Heidebrecht, K. B., Shapiro, A. T., Barloon, P. J., & Goetz, A. F. H. (1993). The Spectral Image Processing System (SIPS) — interactive visualisation and analysis of imaging spectrometer data. *Remote Sensing of Environment*, *44*, 145−163.

Leigh, E. G., Jr., Davidar, P., Dick, C. W., Puyravaud, J. P., Terborgh, J., Ter Steege, H., & Wright, S. J. (2004). Why do some tropical forests have so many species of trees? *Biotropica*, *36*, 447−463.

Li, J. (2004). Wavelet-based feature extraction for improved endmember abundance estimation in linear unmixing of hyperspectral signals. *IEEE Transactions on Geoscience and Remote Sensing*, *42*, 644−649.

Li, J., Bruce, L. M., Byrd, J., & Barnett, J. (2001). Automated detection of *Pueraria montana* (kudzu) through Haar analysis of hyperspectral reflectance data. *Proc. IEEE IGARSS*, *Vol. 5*. (pp. 2247−2249).

Lindsay, R. W., Percival, D. B., & Rothrock, D. A. (1996). The discrete wavelet transform and the scale analysis of the surface properties of sea ice. *IEEE Transactions on Geoscience and Remote Sensing*, *34*, 771−787.

Luther, J. E., & Carroll, A. L. (1999). Development of an index of balsam fir vigor by foliar spectral reflectance. *Remote Sensing of Environment*, *69*, 241−252.

Mallat, S. G. (1989). A theory for multiresolution signal decomposition: The wavelet representation. *IEEE Transactions on Pattern Analysis and Machine Intelligence*, *11*, 674−693.

Martin, M. E., & Aber, J. D. (1997). High spectral resolution remote sensing of forest canopy lignin, nitrogen, and ecosystem processes. *Ecological Applications*, *7*, 431−443.

Martin, M. E., Newman, S. D., Aber, J. D., & Congalton, R. G. (1998). Determining forest species composition using high resolution spectral resolution remote sensing data. *Remote Sensing of Environment*, *65*, 249−254.

Niemann, K. O. (1995). Remote sensing of forest stand age using airborne spectrometer data. *Photogrammetric Engineering and Remote Sensing*, *61*, 1119−1127.

Nischan, M. L., Kerekes, J. P., Baum, J. E., & Basedow, R. W. (1999, July 19–24). Analysis of HYDICE noise characteristics and their impact on subpixel object detection. *SPIE Proceedings*, *3753* (Denver, CO, USA).

Peterson, D. L., Aber, J. D., Matson, P. A., Card, D. H., Swanberg, N., Wessman, C., et al. (1988). Remote sensing of forestry canopy and leaf biochemical contents. *Remote Sensing of Environment*, *24*, 85−108.

Portigal, F., Holasek, R., Mooradian, G., Owensby, P., Dickson, M., Fene, M., et al. (1997, July 7–10). *Vegetation classification using red-edge first derivative and green peak statistical moment indices with the Advanced Airborne Hyperspectral Imaging System (AAHIS)Third International Airborne Remote Sensing Conference and Exhibition, Copenhagen, Denmark*, *Vol. II* (pp. 789−797). Ann Arbor, MI: ERIM.

Powell, R. L., Matzke, N., de Souza, C., Jr., Clark, M., Numata, I., Hess, L. L., et al. (2004). Sources of error in accuracy assessment of thematic land-cover maps in the Brazilian Amazon. *Remote Sensing of Environment*, *90*, 221−234.

Price, J. C. (1992). Variability of high-resolution crop reflectance spectra. *International Journal of Remote Sensing*, *14*, 2593−2610.

Price, J. C. (1994). How unique are spectral signatures? *Remote Sensing of Environment*, *49*, 181−186.

Pu, R., & Gong, P. (2004). Wavelet transform applied to EO-1 hyperspectral data for forest LAI and crown closure mapping. *Remote Sensing of Environment*, *91*, 212−224.

Roberts, D. A., Nelson, B. W., Adams, J. B., & Palmer, F. (1998). Spectral changes with leaf aging in Amazon caatinga. *Trees*, *12*, 315−325.

Roberts, D. A., Numata, I., Holmes, K., Batista, G., Krug, T., Moteiro, A., et al. (2002). Large area mapping of land-cover change in Rondônia using multitemporal spectral mixture analysis and decision tree classifiers. *Journal of Geophysical Research-Atmospheres*, *107*(D20), 8073.

Roberts, D. A., Ustin, S. L., Ogunjemiyo, S., Greenberg, J., Dobrowski, S. Z., Chen, J., et al. (2004). Spectral and structural measures of Northwest forest vegetation at leaf to landscape scales. *Ecosystems*, *7*, 545−562.

Sanchez-Azofeifa, G. A., Castro, K., Rivard, B., Kalascka, M., & Harriss, B. (2003). Remote sensing research priorities in tropical dry forest environments. *Biotropica*, *35*(2), 134−142.

Sanchez-Azofeifa, G. A., Harris, R. C., & Skole, D. L. (2001). Deforestation in Costa Rica: A quantitative analysis using remote sensing imagery. *Biotropica*, *33*(3), 378−384.

Sanchez-Azofeifa, G. A., Castro-Esau, K. (submitted for publication). Canopy observations on the hyperspectral properties of a community of tropical dry forest lianas and their host trees. Research Letter. *International Journal of Remote Sensing*.

Schepers, J. S., Blackmer, T. M., Wilhelm, W. W., & Resende, M. (1996). Transmittance and reflectance measurements of corn leaves from plants with different nitrogen and water supply. *Journal of Plant Physiology*, *148*, 523−529.

Shaw, D. T., Malthus, T. J., & Kupiec, J. A. (1998). High-spectral resolution data for monitoring Scots pine (*Pinus sylvestris* L.) regeneration. *International Journal of Remote Sensing*, *19*, 2601−2608.

Steininger, M. K., Tucker, C. J., Townshend, J. R. G., Killeen, T. J., Desch, A., Bell, V., et al. (2001). Tropical deforestation in the Bolivian Amazon. *Environmental Conservation*, *28*(2), 127−134.

Stuntz, S., Simon, U., & Zotz, G. (2002). Rainforest air-condition: The moderating influence of epiphytes on the microclimate in tropical tree crowns. *International Journal of Biometeorology*, *46*, 53−59.

Thenkabail, P. S. (2002). Optimal hyperspectral narrowbands for discriminating agricultural crops. *Remote Sensing Reviews*, *20*(4), 257−291.

Thenkabail, P. S., Enclona, E. A., Ashton, M. S., & Meer, B. V. D. (2004). Accuracy assessments of hyperspectral waveband performance for vegetation analysis applications. *Remote Sensing of Environment*, *91*, 354−376.

Thenkabail, P. S., Smith, R. B., & De-Pauw, E. (2000). Hyperspectral vegetation indices for determining agricultural crop characteristics. *Remote Sensing of Environment*, *71*, 158−182.

Thenkabail, P. S., Smith, R. B., & De-Pauw, E. (2002). Evaluation of narrowband and broadband vegetation indices for determining optimal hyperspectral wavebands for agricultural crop characterization. *Photogrammetric Engineering and Remote Sensing*, *68*(6), 607−621.

Tsai, F., & Philpot, W. D. (1998). Derivative analysis of hyperspectral data. *Remote Sensing of Environment*, *66*, 41−51.

Van Aardt, J. A. N., & Wynne, R. H. (2001). Spectral separability among six southern tree species. *Photogrammetric Engineering and Remote Sensing*, *67*(12), 1367−1375.

Wessman, C. A., Aber, J. D., & Peterson, D. L. (1989). An evaluation of imaging spectrometry for estimating forest canopy chemistry. *International Journal of Remote Sensing*, *10*, 1293−1316.

Wright, S. J. (2002). Plant diversity in tropical forests: A review of mechanisms of species coexistence. *Oecologia*, *130*, 1−14.

Zagolski, F., Pinel, V., Romier, J., Alcayde, D., Gastellu-Etchegorry, J. P., Giordano, G., et al. (1996). Forest canopy chemistry with high spectral resolution remote sensing. *International Journal of Remote Sensing*, *17*, 1107−1128.

Zarco-Tejada, P. J., Pushnik, J. C., Dobrowski, S., & Ustin, S. L. (2003). Steady-state chlorophyll *a* fluorescence detection from canopy derivative reflectance and double-peak red edge effects. *Remote Sensing of Environment*, *84*, 283−294.